

1 Sediment accumulation, rather than  
2 mixing, controls the temporal resolution  
3 of the sedimentological record

4

5 Niklas Hohmann, Utrecht University, The Netherlands. Email: N.H.Hohmann@uu.nl

6 <https://orcid.org/0000-0003-1559-1838>

7 Jack Middelburg, Utrecht University, The Netherlands. <https://orcid.org/0000-0003-3601->

8 [9072](https://orcid.org/0000-0003-3601-9072)

9 Emilia Jarochovska, Utrecht University, The Netherlands. <https://orcid.org/0000-0001-8937->

10 [9405](https://orcid.org/0000-0001-8937-9405)

11 **This paper is a non-peer reviewed preprint that has been submitted to EarthArXiv. It**  
12 **has not undergone peer review and should not be considered a final publication. The**  
13 **findings and conclusions presented here are preliminary and may be subject to change.**

14

## 15 Abstract

16 Sedimentary particles such as organismal remains carry information on the Earth's past. As a  
17 result of mixing in surface sediments, particles of different ages can be found at the same  
18 depth (time-averaging), and particles of identical ages can be found at different stratigraphic  
19 positions (stratigraphic disorder). This results in simultaneous stratigraphic and temporal  
20 blurring of the recorded signal, thus reducing the resolution of the sedimentological record.

21 Here, we draw on a set of observations from modern marine sediments in which the three  
22 principal properties of the surface mixed layer (sediment accumulation, mixing depth, and  
23 bioturbation intensity) have been measured together, allowing us to disentangle their relative  
24 contributions to time-averaging and stratigraphic disorder. We find that sediment  
25 accumulation has the strongest influence on time-averaging in modern marine environments.  
26 Time-averaging increases with water depth, and a sediment layer in deep sea environments  
27 may represent more than 10 kyr of time. In contrast, stratigraphic disorder is controlled by  
28 mixing depth. Surprisingly, particle mixing due to bioturbation has only a weak effect on  
29 stratigraphic disorder and time-averaging, as the majority of modern sediments are already  
30 thoroughly mixed.

31 Our results highlight that age-reversals are a common feature of the sedimentological record  
32 when sampling below decimeter scale and that the physical processes of sediment mixing and  
33 accumulation rather than analytical errors provide an upper limit on the temporal resolution  
34 achievable in Holocene marine records. Time-averaging and stratigraphic disorder are the  
35 result of the same mixing process in the surface mixed layer, and high temporal and  
36 stratigraphic resolution can only be achieved when sediment accumulation is high. Secular  
37 increases in mixing depth could have led to a 10-fold decrease in the temporal resolution of  
38 the sedimentological record across the Phanerozoic.

## 39 Introduction

40 Sedimentary particles, among them fossils, are the building blocks of the geological record.  
41 In reading it, we generally assume superposition: younger sediment is found on top of older  
42 sediment (Steno 1916). Before entering historical records, particles are mixed as they  
43 transition the sediment surface mixed layer (SML), leading to particles of different ages being  
44 buried together. This reduces the temporal resolution, which propagates into all downstream  
45 analyses of the original signal, including paleoenvironmental or evolutionary reconstructions,  
46 chemostratigraphy, age-depth models, and diversity and disparity analyses (Dolman et al.  
47 2021; Hülse et al. 2022; Tomašových et al. 2023).

48 Particle mixing results in two distinct, but related effects that necessitate each other: time-  
49 averaging, where particles of different ages are found in the same sediment layer  
50 (Kowalewski 1996; Tomašových et al. 2022), and stratigraphic disorder, where particles of  
51 the same age are found at different stratigraphic positions (Berger and Heath 1968; Cutler and  
52 Flessa 1990; Flessa et al. 1993). Dating individual shells in Holocene marine environments  
53 (e.g., via radiocarbon or amino acid racemization dating) has shown that both effects are  
54 common, with values of time-averaging of thousands of years, and shells of similar ages  
55 multiple decimeters apart (Flessa and Kowalewski 1994; Kosnik et al. 2007, 2009;  
56 Dominguez et al. 2016; Tomašových et al. 2018, 2022; Berensmeier et al. 2023). For  
57 example, in the Po river prodelta (Northern Adriatic Sea), Tomašových et al. (2018) observed  
58 shells younger than 25 years both at the sediment surface and buried below 1 m, with values  
59 of time-averaging of 50 years (Figure 1 A).

60 Time-averaging and stratigraphic disorder have a profound influence on our interpretation of  
61 the geological record: Time-averaging acts as a low-pass filter on paleo-time series (Kidwell  
62 2013). Stratigraphic disorder implies that the law of superposition, a crucial model

63 assumption for establishing the order of geological events and for age-depth modelling  
64 (Haslett and Parnell 2008; Hohmann et al. 2025), breaks down below a certain physical scale.  
65 Estimating time-averaging and stratigraphic disorder by means of dating individual particles  
66 in a sedimentary layer is labor-intensive and limited to the resolution of radiocarbon dating.  
67 As a result, researchers lack methods to easily assess the resolution of their records,  
68 particularly in the pre-Quaternary. Here we refer to resolution as the depositional resolution  
69 of an unbedded sedimentological record, i.e. not the stratigraphic resolution that is the  
70 property of a bedded (discrete) record (sensu Kowalewski and Bambach (2003)). Particle  
71 mixing in the SML is controlled by sedimentological and ecological parameters such as  
72 mixing depth, bioturbation intensity, and sediment accumulation rate. Values of SML  
73 parameters are characteristic for specific depositional environments, and their change  
74 throughout the Phanerozoic has been documented (Tarhan 2018; Zhang et al. 2024; Tarhan et  
75 al. 2025). Here we use a diffusion-advection model to predict time-averaging and  
76 stratigraphic disorder from SML parameters. This opens the opportunity to estimate the  
77 resolution of the sedimentological record from extrinsic, empirically traceable factors.

78 We establish the connection between time-averaging, stratigraphic disorder, and SML  
79 parameters (mixing depth, bioturbation intensity, and sediment accumulation). Surprisingly,  
80 we find that sediment accumulation, not bioturbation intensity, is the dominant control of the  
81 temporal resolution in modern marine sediments. Sediment accumulation is a predictor of  
82 temporal resolution in environments for periods where direct assessments of time-averaging  
83 are impossible. Stratigraphic disorder and time-averaging are equivalent expressions of  
84 mixing in the SML, and records having both high temporal resolution (low time-averaging)  
85 and high stratigraphic resolution (low stratigraphic disorder) require high accumulation  
86 settings. In deep time, our model predicts a 10-fold decrease in temporal resolution over the  
87 Phanerozoic due to secular increases in mixing depth with progressive infaunalization.

## 88 Methods

89 We model the joint distribution of particle ages and depths via the diffusion-advection  
90 equation

$$91 \quad \frac{\partial}{\partial a} u(a, d) = \frac{\partial}{\partial d} \left( D_b(d) \frac{\partial}{\partial d} u(a, d) - Su(a, d) \right) \text{ (Eq. 1)}$$

92 where  $a$  is particle age,  $d$  is depth below the sediment-water interface,  $u(a, d)$  is the density  
93 of particles of age  $a$  at depth  $d$ ,  $S$  is sediment accumulation rate, and  $D_b$  is the depth-  
94 dependent biodiffusion coefficient (Figure 1 B). This model is based on the classic Guinasso  
95 and Schink (1975) model, see Hohmann (2024) for the model derivation and Terry and  
96 Novak (2015) for a similar model in cave environments. It assumes particles are abundant  
97 and sediment mixing due to bioturbation can be approximated as biodiffusion (Meysman et  
98 al. 2010; Kuderer 2022). For the boundary conditions, we assume particles of age 0 are  
99 introduced at the sediment surface, mixed and advected in the surface mixed layer (SML), do  
100 not exit at the sediment-water interface, and are eventually exported into historical sediment  
101 layers below the SML (maturation depth sensu Sadler (1993)) (see Supplementary  
102 Information).

103 To inform the model using compilations of SML parameters from modern marine  
104 environments, we assume biodiffusion  $D_b$  is constant within a SML of thickness  $L$  and drops  
105 to 0 below (Hohmann 2022). To reduce the parameter space and facilitate numeric stability,  
106 we re-scale the system using mixing depth  $L$  as characteristic length unit and  $L/S$  (transit time  
107 of particles through the SML due to sediment accumulation) as characteristic time unit. The  
108 re-scaled system is fully characterized by the dimensionless mixing intensity (inverse Péclet  
109 number)

110 
$$G = \frac{D_b}{L \cdot S} \text{ (Eq. 2)}$$

111 (Guinasso and Schink 1975), which represents the importance of mixing relative to  
112 (advective) burial in particle transport. We measure time-averaging *avg* and stratigraphic  
113 disorder *disord* using the interquartile range of particle ages and depths, respectively  
114 (Tomašových et al. 2018; Berensmeier et al. 2023). Let  $F_{mix}(G)$  be time-averaging in the  
115 rescaled system as a function of mixing intensity. Reversing the scaling, we get

116 
$$avg = F_{mix}(G) \cdot \frac{L}{S} \text{ and } disord = F_{mix}(G) \cdot L \text{ (Eq. 3)}$$

117 for time-averaging and stratigraphic disorder, yielding the relation

118 
$$avg \cdot S = disord \text{ (Eq. 4)}$$

119 between the two (see Supplementary Information, Supplementary Figure 1). Values of  $F_{mix}$   
120 were calculated using Matlab (MATLAB R2025b) for values of  $G$  between  $10^{-3}$  and  $10^5$   
121 (Figure 2), all other analyses were performed in the R language version 4.5.3 (R Core Team  
122 2026), see Supplementary Information and Code for details.

123 We calculate time-averaging and stratigraphic disorder for locations in the SMLBase, a global  
124 compilation of 287 simultaneous co-located measurements of  $D_b$ ,  $S$ , and  $L$  in modern marine  
125 sediments based on tracer profiles (Hohmann (2022), Supplementary Figure 2). We consider  
126 an environment to be saturated with respect to mixing when  $F_{mix}$  is within 90 % of the  
127 maximum  $F_{mix}$  achievable, i.e., when  $F_{mix} > 0.989$  (Figure 2, Supplementary Figure 2 D).  
128 We use two generalized linear models (GLMs) with identity linkage function to examine the  
129 relationship between  $D_b$ ,  $S$ , and  $L$  (independent variables) and time-averaging and  
130 stratigraphic disorder (dependent variables). For the GLMs, we determine partial  $R^2$ , where a  
131 large value indicates a strong relationship, and the regression and standardized regression

132 coefficients, where a high value reflects that a change in the independent variable results in a  
133 large change in the dependent variable (Figure 3, Supplementary Tables 1 and 2,  
134 Supplementary Figure 3). In addition, we examine how time-averaging and stratigraphic  
135 disorder change along a water depth gradient (Figure 4).

## 136 Results

137 We find that sediment accumulation rate is the dominant control on the temporal resolution of  
138 the sedimentological record (regression coefficient -1.057, standardized reg. coefficient -  
139 0.991, partial  $R^2$  0.995, Figure 3 A-C, Supplementary Table 1, Supplementary Figure 3).

140 Halving the sediment accumulation rate roughly doubles the temporal resolution of the  
141 sedimentological record, as measured by time-averaging (interquartile range of particle ages  
142 found within the same sediment layer (Tomašových et al. 2018)). Time-averaging reaches  
143 values as high as 10 kyr in deep-sea settings (Figure 4 A, Supplementary Table 3).

144 Below decimeter resolution, the law of superposition begins to break down due to  
145 stratigraphic disorder, with mixing depth being the major determinant of disorder (regression  
146 coefficient 0.931, standardized reg. coefficient 0.949, partial  $R^2$  0.981, Figure 3 D-F,  
147 Supplementary Table 2, Supplementary Figure 3). When sampling below this resolution,  
148 recovery of true age reversals (finding older particles stratigraphically higher than younger  
149 ones) will be common, and reducing sampling resolution further will not improve the  
150 temporal resolution of the recovered record.

151 Counterintuitively, bioturbation intensity as expressed by the biodiffusion coefficient has only  
152 a weak effect on time-averaging and stratigraphic disorder (time-averaging: regression  
153 coefficient 0.063, standardized reg. coefficient 0.078, partial  $R^2$  0.569, stratigraphic disorder:

154 regression coefficient 0.063, standardized reg. coefficient 0.227, partial  $R^2$  0.569, Figure 3 B,  
155 E, Supplementary Tables 1 and 2, Supplementary Figure 3).

156 We found that environments with mixing intensity  $G$  larger than 1.56 (Péclet number below  
157 0.64) are saturated with respect to mixing (Figure 2). In these environments, time-averaging  
158 and stratigraphic disorder are dominated by the physical dimensions of the surface mixed  
159 layer (mixing depth and transit time due to sediment accumulation) rather than variations in  
160 mixing (Equation 3). Of the 287 modern sediments included in the analysis, 79 % are  
161 saturated with respect to mixing (Figure 2, Supplementary Figure 2 D). This explains the  
162 results of our regression analysis (see above), where time-averaging and stratigraphic  
163 disorder are controlled by sediment accumulation rate or mixing depth rather than the  
164 biodiffusion coefficient.

165 Time-averaging and stratigraphic disorder are related through the sediment accumulation rate  
166 (Equation 4), demonstrating that both parameters are equivalent manifestations of particle  
167 mixing in the surface sediments. Records having both high temporal and stratigraphic  
168 resolution (low stratigraphic disorder and time-averaging) can only be achieved in high  
169 sediment-accumulation settings.

## 170 Discussion

171 As first-order approximation, we found that time-averaging in modern marine sediments is  
172 approximately equal to the particle residence time in the surface mixed layer (SML)

$$173 \quad t_{avg} \approx \frac{L}{S} \text{ (Eq. 5)}$$

174 (compare Delhez and Deleersnijder (2012)) and stratigraphic disorder is approximately equal  
175 to the mixing depth:

176

$$disord \approx L \text{ (Eq. 6).}$$

177 These approximations hold because most modern environments (79 %) are thoroughly mixed,  
178 and minor variations in mixing intensity will, accordingly, not impact time-averaging and  
179 stratigraphic disorder (Figure 2, Equation 3). Commonly, systems with mixing intensity  $G$   
180 larger than 10 (Péclet number  $Pe$  below 0.1) are considered dominated by mixing  
181 (Wheatcroft 1990; Kuderer and Middelburg 2024). Our study identifies environments with a  
182 mixing intensity  $G$  larger than 1.56 (or, equivalent,  $Pe < 0.64$ ) as thoroughly mixed based  
183 on a comparison with the maximum achievable time-averaging and disorder. This shows that  
184 even moderate biodiffusion values are sufficient to result in a mixing-dominated SML, in  
185 which increases in mixing do not result in more time-averaging or stratigraphic disorder.

186 On a global average, mixing depth is approximately 10 cm in modern sediments (Boudreau  
187 1994, 1998) and correlates positively with measures of food availability, such as seafloor  
188 organic carbon availability and macrofauna biomass, but not water depth or sediment  
189 accumulation rate (Teal et al. 2010; Zhang et al. 2024). Stratigraphic disorder of  
190 approximately 10 cm should thus be the null expectation for modern sediments. Nonetheless,  
191 significant local deviations from this prediction are possible. Hypoxic conditions can reduce  
192 both bioturbation depth and intensity (Smith et al. 2000; Sturdivant et al. 2012). While  
193 reduced mixing depth will improve the resolution of sedimentary records of sediment  
194 underlying low-oxygen bottom waters, the total effect depends on how the decreases of  
195 bioturbation and mixing depth balance out in  $G$ . Similar considerations hold for  
196 extrapolations into deep time or into the future. Humans modify the seafloor in a plethora of  
197 ways, which can change mixing depth, sediment accumulation rate, and biodiffusion - and, as  
198 a result, time-averaging and stratigraphic disorder - in all directions (Tomašových et al. 2018;  
199 Berensmeier et al. 2023; Nawrot et al. 2024).

200 While infaunalization emerged early in the Paleozoic, the development of a well-mixed

201 sediment surface layer lagged, and mixing depths only gradually increased (Seilacher et al.  
202 2005; Tarhan et al. 2015; Tarhan 2018). This suggests that time-averaging and stratigraphic  
203 disorder increased throughout the Paleozoic in parallel with the rise of bioturbators (Kidwell  
204 1997; Tomašových et al. 2024). Inference of paleo-mixing depths is challenging and  
205 associated with large uncertainties (Buatois et al. 2025). Quantitatively, our Equation 3  
206 predicts that the 10-fold increase in mixing depth across the Phanerozoic reported by Tarhan  
207 et al. (2015) would result in an increase of time-averaging and stratigraphic disorder by an  
208 order of magnitude (given the SML remained well-mixed).

209 Sediment accumulation rate negatively correlates with water depth, and has an indirect  
210 influence on biodiffusion intensity by delivering organic matter (Middelburg et al. 1997;  
211 Zhang et al. 2024). Combined, this suggests that both water depth and sediment accumulation  
212 rates can be used as an (external) taphonomic clock to estimate the temporal resolution of  
213 depositional environments for which no direct estimates of time-averaging are available  
214 (Kidwell 1997; Immenhauser 2009; Tomašových et al. 2017). In the rock record, estimates of  
215 accumulation rate decrease with the period of observation (Sadler 1981) and in sections  
216 without good age control it will be often impossible to calculate this rate at the timescale  
217 comparable to the transit time of a particle through the SML. However, when short-term  
218 accumulation rates are available, they correlate negatively with time-averaging, providing an  
219 empirical support to our model results (Meldahl et al. 1997).

220 It is well-established that sediment mixing acts as a low-pass filter on pre-diagenetic  
221 geological signals, smoothing out signals below a certain frequency via time-averaging  
222 (Olszewski 1999; Kanzaki et al. 2021; Hülse et al. 2022; Kuderer 2022). This can both  
223 remove a signal of interest (e.g., precession, Hülse et al. (2022)) or help focus on long-term  
224 baselines by removing noise below the timescale of interest (Kowalewski et al. 1998; Kidwell  
225 2013). Depositional environments are characterized by a range of typical sediment

226 accumulation rates, and, as a result, can be assigned characteristic values of time-averaging  
227 and an associated cutoff frequency of a low-pass filter. This connection can serve as a  
228 heuristic to determine depositional environments suitable to record a signal of interest. For  
229 example, intermediate accumulation rate settings are more suitable for establishing pre-  
230 anthropogenic baselines for conservation paleobiology, while settings with rapid  
231 accumulation are more suitable to study deep-time analogues for climate change in high  
232 resolution. However, high sediment accumulation rate environments are usually near-shore  
233 and thus prone to erosion (Sommerfield 2006), indicating that there might be a fundamental  
234 trade-off between stratigraphic completeness and the maximum achievable temporal  
235 resolution.

236 We find a strong connection between time-averaging and stratigraphic disorder, as they can  
237 be transformed into each other by multiplication with the sediment accumulation rate  
238 (Equation 4). This is a direct consequence of purely advective particle transport below the  
239 mixed layer (Supplementary Figure 1, Supplementary Equations 5 to 7). As such, it is  
240 independent of how the SML is modeled and will similarly hold for complex, multimodal  
241 distributions of particle ages. Equation 4 makes the suspected connection between time-  
242 averaging and disorder (e.g., Kowalewski (1996)) explicit and allows to estimate disorder by  
243 means of time-averaging and sediment accumulation rate, data that is more easily traceable  
244 empirically (e.g., Tomašových et al. (2018)). A well-ordered record with high temporal  
245 resolution (low values of both time-averaging and stratigraphic disorder) is highly desirable  
246 for any study relying on paleorecords. Our results formalize why these records are most  
247 likely found in high-sedimentation environments.

248 The law of superposition is a core principle of geology, frequently used as model assumption  
249 in geochronology or to establish ordering of events in the absence of age constraints. Age-  
250 depth modeling methods assume the age of a sediment layer can be known exactly given

251 sufficient high-resolution data, and they typically enforce the law of superposition when  
252 faced with age-reversals (Haslett and Parnell 2008; Hohmann et al. 2025). Our results  
253 highlight that, below the physical scale of stratigraphic disorder and time-averaging, sediment  
254 layers do not have a single, well-defined age. On this scale, the physical processes of  
255 sediment deposition and mixing introduce irreducible uncertainty into age-depth relationships  
256 that cannot be resolved with the addition of more, high-resolution data. Palaeoecological  
257 studies frequently report time-averaging above 1000 years (Flessa and Kowalewski 1994;  
258 Scarponi et al. 2017; Tomašových et al. 2018; Berensmeier et al. 2023), an order of  
259 magnitude larger than the age-uncertainty of dating individual particles (e.g., via radiocarbon  
260 or amino acid racemization dating (Hajdas et al. 2021)) and stratigraphic disorder on the  
261 decimeter scale (Flessa et al. 1993; Kosnik et al. 2007, 2009; Dominguez et al. 2016;  
262 Tomašových et al. 2018). Not dating precision, but age uncertainty introduced by time-  
263 averaging will be the limiting factor for age-depth modelling in low-accumulation (sediment  
264 accumulation below 0.01 cm/y) Holocene environments (Kowalewski et al. 1998; Dolman et  
265 al. 2021).

266 Our model assumptions of constant sediment accumulation, biodiffusion, and mixing depth  
267 reflect data availability from compilations of empirical measurements and the standard  
268 approaches used to estimate SML parameters from tracer profiles. While there are multiple  
269 global compilations of individual SML parameters available (e.g., Song et al. (2022); Solan et  
270 al. (2019)), we use a compilation containing all three parameters of interest measured at the  
271 same location to avoid propagation of extrapolation effects into our results (Hohmann 2022).  
272 We hypothesize that episodic sediment accumulation will reduce time-averaging and disorder  
273 by removing particles from the SML faster, thus reducing their exposure to mixing (Sadler  
274 1993). Deep mixing below the recognized mixing depth will, however, increase time-  
275 averaging (Tomašových et al. 2023) and, as a result, stratigraphic disorder.

276 Many models of particle mixing and its effect on earth science signals are available in the  
277 scientific literature, allowing for modeling of complex depth- and time-dependent dynamics  
278 (see e.g., Meysman et al. (2010)). The majority of SML parameters are estimated by fitting  
279 tracer profiles predicted by the Guinasso and Schink (1975) model to empirical observations  
280 (e.g., DeMaster and Cochran (1982)). As the diffusion-advection model used here is also  
281 derived from the Guinasso and Schink model, it minimizes discrepancies between inference  
282 and prediction models while remaining simple enough to provide analytical insights into the  
283 connection between particle age and depth (e.g., Equations 3 and 4).

284 Biodiffusion can be anisotropic (Wheatcroft 1991), spatially heterogeneous (Zuhr et al. 2022)  
285 and size-dependent (Wheatcroft and Jumars 1987; Shull and Yasuda 2001; Hupp et al. 2019;  
286 Hupp and Kelly 2020) due to ecological preferences of bioturbators and physical effects such  
287 as granular convection (Savranskaia et al. 2022). Higher biodiffusion coefficients have been  
288 observed in the fine particle fraction (Wheatcroft and Jumars 1987), suggesting that time-  
289 averaging and disorder might be reduced for large particles. However, it is common to  
290 observe high values of stratigraphic disorder and age-homogenization across multiple  
291 decimeters for large shells (fraction > 4 mm) (Kosnik et al. 2007, 2009; Dominguez et al.  
292 2016; Tomašových et al. 2018). This suggests that while mixing intensity of large particles is  
293 high enough for our results to be valid for large size fractions, the exact values of time-  
294 averaging and stratigraphic disorder might vary across size fractions.

295 Destruction of particles in the taphonomic active zone (Davies et al. 1989) reduces time-  
296 averaging (Kowalewski 1996; Olszewski 2004; Kowalewski et al. 2017), and, as a result,  
297 stratigraphic disorder. Our model does not incorporate particle destruction, as the taphonomic  
298 half-life of particles encapsulates age- and taxon-dependent dissolution of (bio)minerals,  
299 sequestration, and loss of taxonomically identifiable features and is accordingly difficult to  
300 constrain (Davies et al. 1989; Meldahl et al. 1997; Kidwell et al. 2005; Tomašových et al.

301 2014; Kowalewski et al. 2017; Nawrot et al. 2022). Our estimates are applicable to particles  
302 with a taphonomic half-life longer than the particle residence time in the taphonomically  
303 active zone (Delhez and Deleersnijder 2012). Especially in deep-sea environments with very  
304 high predicted values of time-averaging, taphonomic half-life will become a limiting factor  
305 (Kuderer and Middelburg 2024). Particle destruction will also reduce sample size, increasing  
306 the effects of random fluctuations (Olszewski 2004). However, the interquartile range is  
307 robust to outliers, reducing the effect of small sample sizes and reworking of exceptionally  
308 old particles.

## 309 Conclusions

310 Informing a model of the surface mixed layer with parameters measured in modern  
311 environments, we found sediment accumulation has the strongest effect on the temporal  
312 resolution of the sedimentary record as expressed by time-averaging of particles, attaining  
313 values higher than 10 kyr in deep-sea settings. The law of superposition breaks down below  
314 decimeter scale due to stratigraphic disorder, which is controlled by mixing depth. Secular  
315 increases in mixing depth might have resulted in a 10-fold decrease in temporal resolution  
316 throughout the Phanerozoic.

## 317 Code and data availability

318 All code required to reproduce the results is available under  
319 <https://doi.org/10.5281/zenodo.20813310> (Hohmann 2026), supplementary information is  
320 archived under <https://doi.org/10.5281/zenodo.20813575> (Hohmann and Jarochovska 2026).

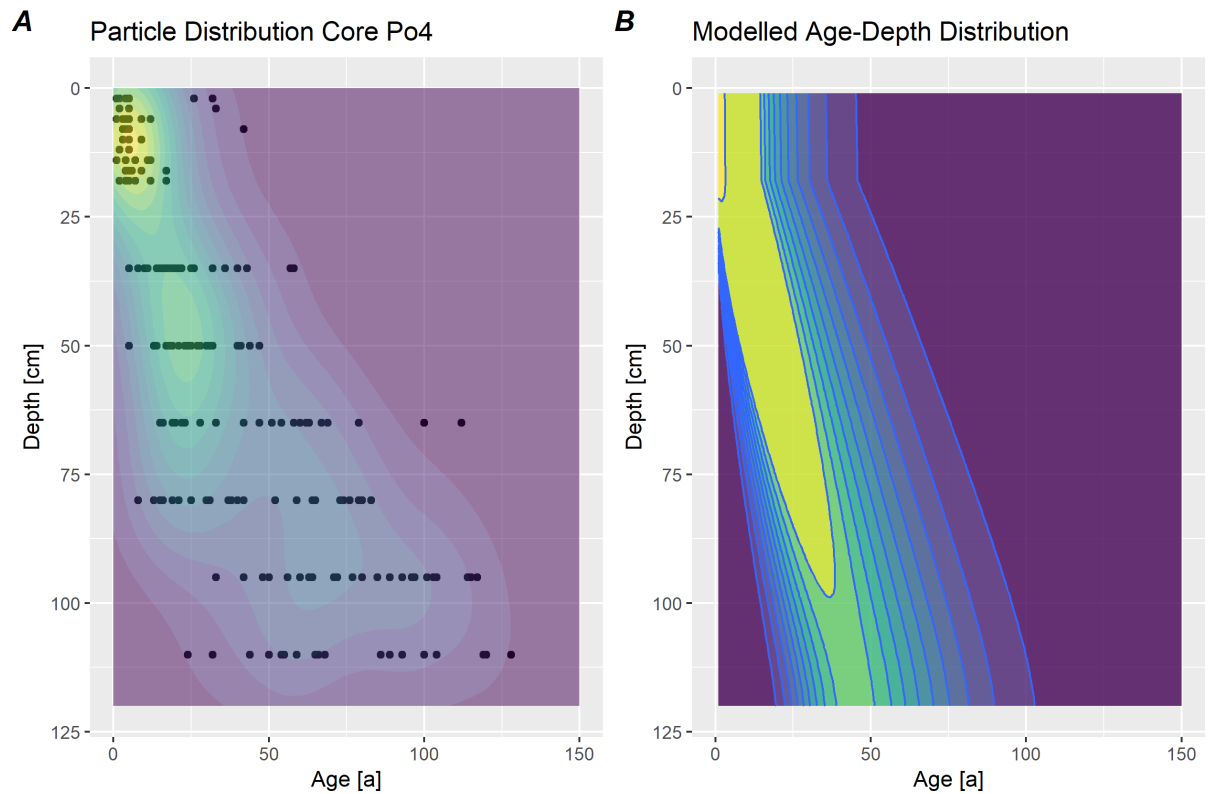
## 321 Author contributions

322 NH: Conceptualization, Formal analysis, Investigation, Methodology, Software, Validation,  
323 Visualization, Writing (original draft, review and editing). JM: Writing (review and editing).  
324 EJ: Conceptualization, Funding acquisition, Validation, Supervision, Writing (review and  
325 editing).

## 326 Funding information

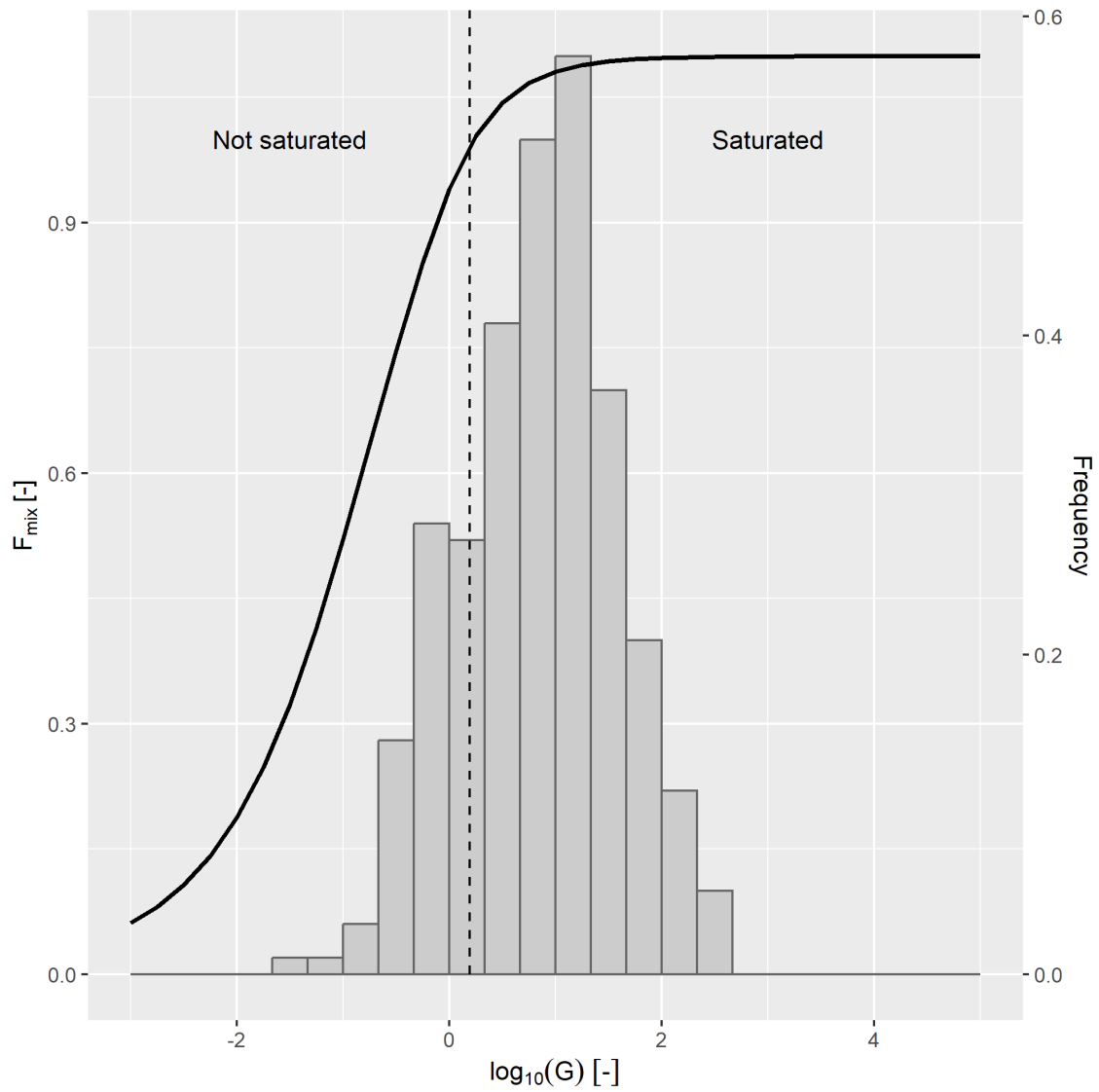
327 Funded by the European Union (ERC, MindTheGap, StG project no 101041077). Views and  
328 opinions expressed are however those of the author(s) only and do not necessarily reflect  
329 those of the European Union or the European Research Council. Neither the European Union  
330 nor the granting authority can be held responsible for them.

331 **Figures**



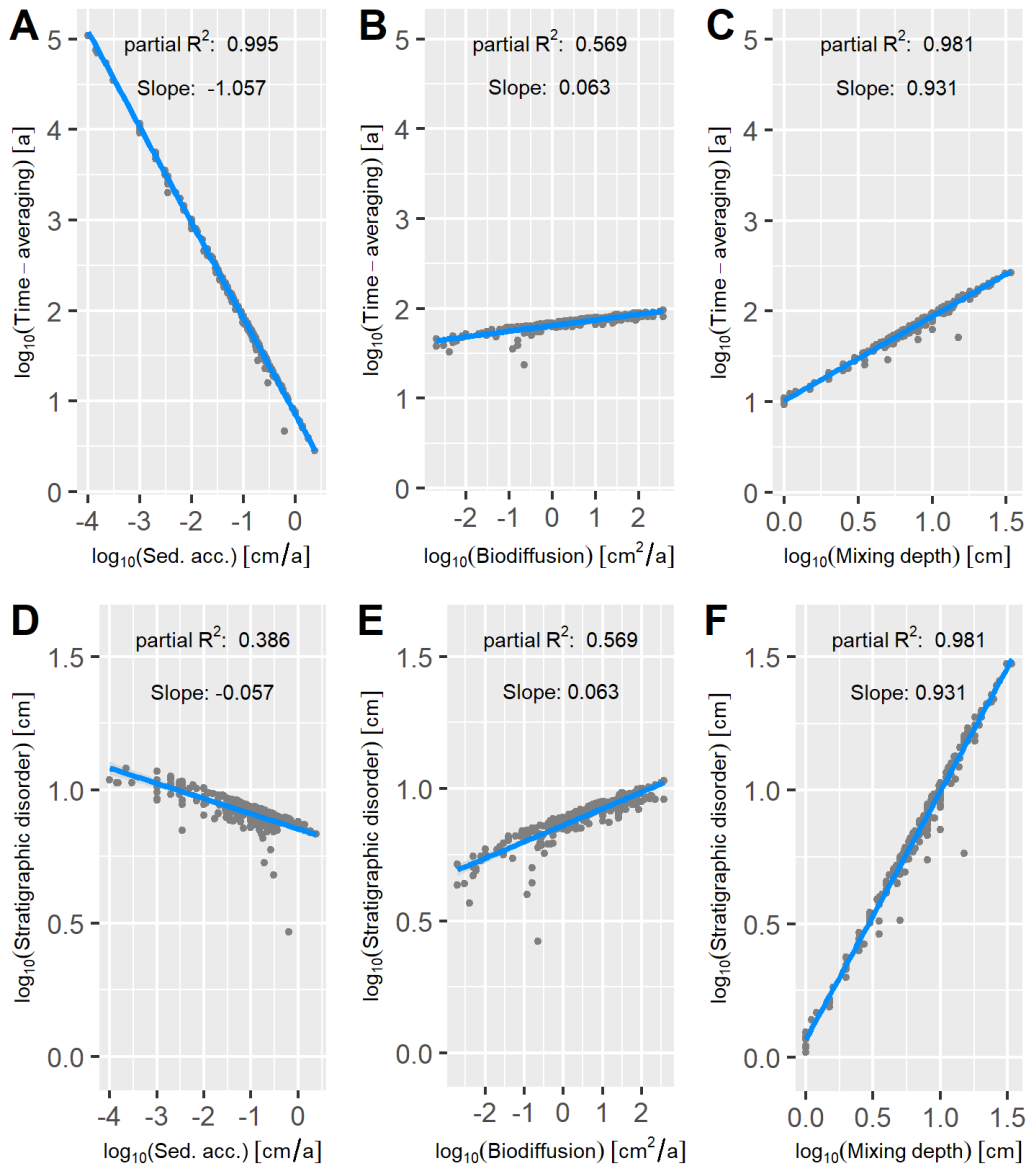
332

333 *Figure 1: Age-depth distribution (A) of 221 individually dated shells of the bivalve Corbula*  
334 *gibba from the Po prodelta, Northern Adriatic Sea (Tomašových et al. 2018) and their density*  
335 *estimate (B) approximated with the diffusion-advection equation used in this study (Equation*  
336 *1, see Supplementary Information for details). Time-averaging of C. gibba at 95 cm is 49*  
337 *years (interquartile range), shells younger than 25 years can be found both at the surface and*  
338 *buried below 1 m.*



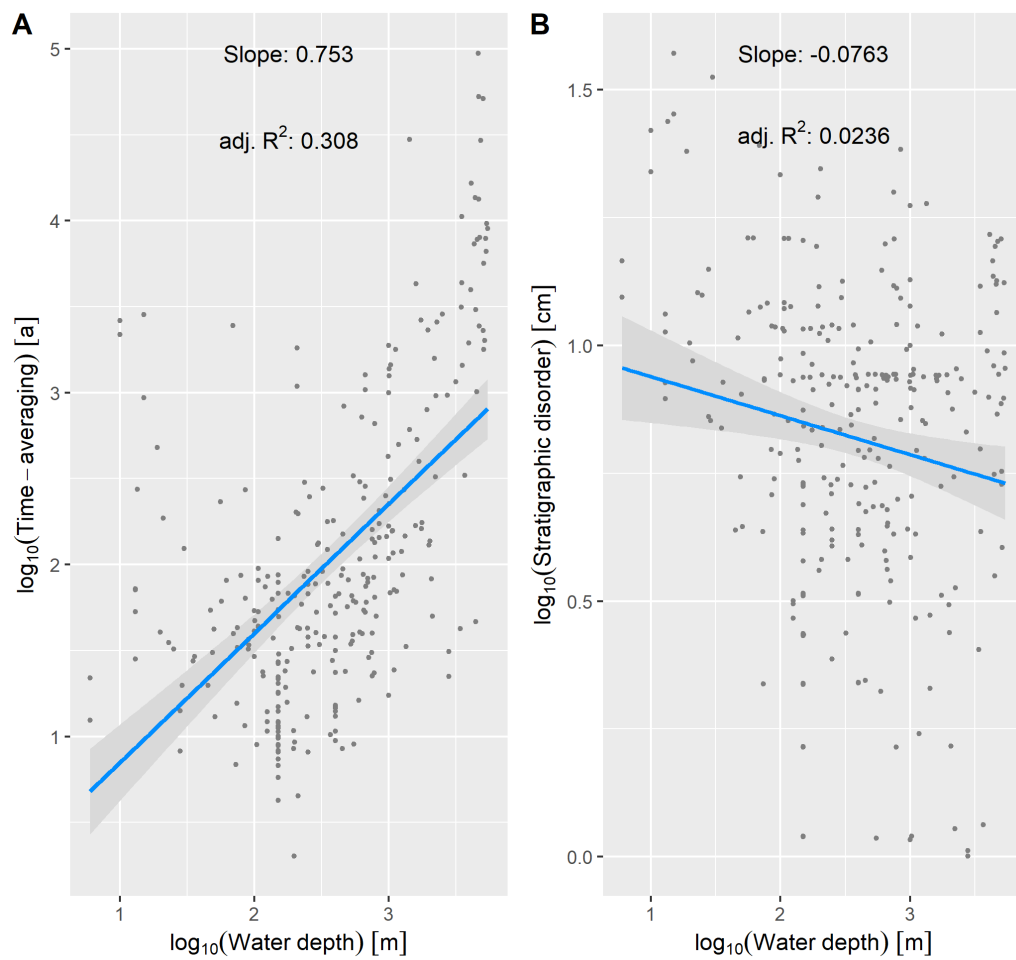
339

340 *Figure 2 Time-averaging  $F_{mix}$  in the rescaled system as a function of mixing intensity  $G$*   
 341 *(black) and histogram of  $G$  in the SMLBase informing the regression analysis (Hohmann*  
 342 *2022). A total of 287 observations are included, the majority (79 %) are saturated with*  
 343 *respect to mixing (see also Supplementary Figure 2 D).*



344

345 *Figure 3: Time-averaging (top row) and stratigraphic disorder (bottom row) in dependence*  
 346 *of sediment accumulation rate  $S$  (A, D), mixing depth  $L$  (B, E) and biodiffusion  $D_b$  (C, F).*  
 347 *Sample size is  $n = 287$ , standard errors,  $p$ -values, and standardized regression coefficients*  
 348 *are reported in Supplementary Tables 1 and 2. Partial  $R^2$  and slope of mixing depth and*  
 349 *biodiffusion are identical in both GLMs due to their analytical connection (Equation 4).*



350

351 *Figure 4: Water depth versus time-averaging (A) and stratigraphic disorder (B). Sample size*  
 352 *is  $n = 287$ , full results of the regression analysis are reported in Supplementary Table 3.*

- 354 Berensmeier, Michaela, Adam Tomašových, Rafat Nawrot, et al. 2023. “Stratigraphic Expression  
355 of the Human Impacts in Condensed Deposits of the Northern Adriatic Sea.” *Geological*  
356 *Society, London, Special Publications* 529 (1): 195–222. [https://doi.org/10.1144/SP529-](https://doi.org/10.1144/SP529-2022-188)  
357 [2022-188](https://doi.org/10.1144/SP529-2022-188).
- 358 Berger, Wolfgang, and G. Heath. 1968. “Vertical Mixing in Pelagic Sediments.” *Journal of Marine*  
359 *Research* 26 (2). [https://elischolar.library.yale.edu/journal\\_of\\_marine\\_research/1122](https://elischolar.library.yale.edu/journal_of_marine_research/1122).
- 360 Boudreau, Bernard P. 1994. “Is Burial Velocity a Master Parameter for Bioturbation?”  
361 *Geochimica et Cosmochimica Acta* 58 (4): 1243–49. [https://doi.org/10.1016/0016-](https://doi.org/10.1016/0016-7037(94)90378-6)  
362 [7037\(94\)90378-6](https://doi.org/10.1016/0016-7037(94)90378-6).
- 363 Boudreau, Bernard P. 1998. “Mean Mixed Depth of Sediments: The Wherefore and the Why.”  
364 *Limnology and Oceanography* 43 (3): 524–26.  
365 <https://doi.org/10.4319/lo.1998.43.3.0524>.
- 366 Buatois, Luis A., M. Gabriela Mángano, Romain Gougeon, et al. 2025. “Biogenic Sediment  
367 Mixing: Bridging the Gap Between the Modern and the Ancient.” *PALAIOS* 40 (9): 248–57.  
368 <https://doi.org/10.2110/palo.2025.011>.
- 369 Cutler, Alan H., and Karl W. Flessa. 1990. “Fossils out of Sequence; Computer Simulations and  
370 Strategies for Dealing with Stratigraphic Disorder.” *PALAIOS* 5 (3): 227–35.  
371 <https://doi.org/10.2307/3514941>.
- 372 Davies, David J., Eric N. Powell, and Robert J. Stanton Jr. 1989. “Relative Rates of Shell  
373 Dissolution and Net Sediment Accumulation - a Commentary: Can Shell Beds Form by  
374 the Gradual Accumulation of Biogenic Debris on the Sea Floor?” *Lethaia* 22 (2): 207–12.  
375 <https://doi.org/10.1111/j.1502-3931.1989.tb01683.x>.
- 376 Delhez, Éric J. M., and Éric Deleersnijder. 2012. “Residence and Exposure Times : When  
377 Diffusion Does Not Matter.” *Ocean Dynamics* 62 (10): 1399–407.  
378 <https://doi.org/10.1007/s10236-012-0568-y>.
- 379 DeMaster, David J., and J. Kirk Cochran. 1982. “Particle Mixing Rates in Deep-Sea Sediments  
380 Determined from Excess 210Pb and 32Si Profiles.” *Earth and Planetary Science Letters*  
381 61 (2): 257–71. [https://doi.org/10.1016/0012-821X\(82\)90057-7](https://doi.org/10.1016/0012-821X(82)90057-7).
- 382 Dolman, Andrew M., Jeroen Groeneveld, Gesine Mollenhauer, Sze Ling Ho, and Thomas  
383 Laepple. 2021. “Estimating Bioturbation From Replicated Small-Sample Radiocarbon  
384 Ages.” *Paleoceanography and Paleoclimatology* 36 (7): e2020PA004142.  
385 <https://doi.org/10.1029/2020PA004142>.
- 386 Dominguez, J. Gabriel, Matthew A. Kosnik, Andrew P. Allen, et al. 2016. “Time-Averaging and  
387 Stratigraphic Resolution in Death Assemblages and Holocene Deposits: Sydney  
388 Harbour’s Molluscan Record.” *PALAIOS* 31 (11): 563–74.  
389 <https://doi.org/10.2110/palo.2015.087>.
- 390 Flessa, Karl W., Alan H. Cutler, and Keith H. Meldahl. 1993. “Time and Taphonomy: Quantitative  
391 Estimates of Time-Averaging and Stratigraphic Disorder in a Shallow Marine Habitat.”  
392 *Paleobiology* 19 (2): 266–86. <https://doi.org/10.1017/S0094837300015918>.
- 393 Flessa, Karl W., and Michal Kowalewski. 1994. “Shell Survival and Time-Averaging in Nearshore  
394 and Shelf Environments: Estimates from the Radiocarbon Literature.” *Lethaia* 27 (2):  
395 153–65. <https://doi.org/10.1111/j.1502-3931.1994.tb01570.x>.
- 396 Guinasso, N. L., and D. R. Schink. 1975. “Quantitative Estimates of Biological Mixing Rates in  
397 Abyssal Sediments.” *Journal of Geophysical Research (1896-1977)* 80 (21): 3032–43.  
398 <https://doi.org/10.1029/JC080i021p03032>.
- 399 Hajdas, Irka, Philippa Ascough, Mark H. Garnett, et al. 2021. “Radiocarbon Dating.” *Nature*  
400 *Reviews Methods Primers* 1 (1): 1–26. <https://doi.org/10.1038/s43586-021-00058-7>.

401 Haslett, John, and Andrew Parnell. 2008. "A Simple Monotone Process with Application to  
402 Radiocarbon-Dated Depth Chronologies." *Journal of the Royal Statistical Society Series*  
403 *C: Applied Statistics* 57 (4): 399–418. <https://doi.org/10.1111/j.1467-9876.2008.00623.x>.

404 Hohmann, Niklas. 2022. "Global Compilation of Surface Mixed Layer Parameters  
405 (Sedimentation Rate, Bioturbation Depth, Mixing Intensity) from Marine Environments:  
406 The SMLBase v1.0." *Frontiers in Earth Science* 10 (December): 1013174.  
407 <https://doi.org/10.3389/feart.2022.1013174>.

408 Hohmann, Niklas. 2024. *PartiMoDe: Modeling Particle Movement and Destruction in the*  
409 *Sediment Surface Mixed Layer*. V. v1.0.0. Zenodo, released August 2.  
410 <https://doi.org/10.5281/ZENODO.13169644>.

411 Hohmann, Niklas. 2026. *Sediment Accumulation, Rather than Mixing, Controls the Temporal*  
412 *Resolution of the Sedimentological Record: Supplementary Code*. V. 1.0.1. Zenodo,  
413 released June 23. <https://doi.org/10.5281/ZENODO.20813310>.

414 Hohmann, Niklas, David De Vleeschouwer, Sietske Batenburg, and Emilia Jarochovska. 2025.  
415 "Nonparametric Estimation of Age–Depth Models from Sedimentological and  
416 Stratigraphic Information." *Geochronology* 7 (3): 427–48.  
417 <https://doi.org/10.5194/gchron-7-427-2025>.

418 Hohmann, Niklas, and Emilia Jarochovska. 2026. *Sediment Accumulation, Rather than Mixing,*  
419 *Controls the Temporal Resolution of the Sedimentological Record: Supplementary*  
420 *Information*. Version 1.0.0. June 23. <https://doi.org/10.5281/ZENODO.20813575>.

421 Hülse, Dominik, Pam Vervoort, Sebastiaan J. van de Velde, et al. 2022. "Assessing the Impact of  
422 Bioturbation on Sedimentary Isotopic Records through Numerical Models." *Earth-*  
423 *Science Reviews* 234 (November): 104213.  
424 <https://doi.org/10.1016/j.earscirev.2022.104213>.

425 Hupp, Brittany, and D. Clay Kelly. 2020. "Delays, Discrepancies, and Distortions: Size-  
426 Dependent Sediment Mixing and the Deep-Sea Record of the Paleocene-Eocene  
427 Thermal Maximum From ODP Site 690 (Weddell Sea)." *Paleoceanography and*  
428 *Paleoclimatology* 35 (11): e2020PA004018. <https://doi.org/10.1029/2020PA004018>.

429 Hupp, Brittany N., D. Clay Kelly, James C. Zachos, and Timothy J. Bralower. 2019. "Effects of  
430 Size-Dependent Sediment Mixing on Deep-Sea Records of the Paleocene-Eocene  
431 Thermal Maximum." *Geology* 47 (8): 749–52. <https://doi.org/10.1130/G46042.1>.

432 Immenhauser, Adrian. 2009. "Estimating Palaeo-Water Depth from the Physical Rock Record."  
433 *Earth-Science Reviews* 96 (1): 107–39. <https://doi.org/10.1016/j.earscirev.2009.06.003>.

434 Kanzaki, Yoshiki, Dominik Hülse, Sandra Kirtland Turner, and Andy Ridgwell. 2021. "A Model for  
435 Marine Sedimentary Carbonate Diagenesis and Paleoclimate Proxy Signal Tracking: IMP  
436 v1.0." *Geoscientific Model Development* 14 (10): 5999–6023.  
437 <https://doi.org/10.5194/gmd-14-5999-2021>.

438 Kidwell, Susan M. 1997. "Time-Averaging in the Marine Fossil Record: Overview of Strategies and  
439 Uncertainties." *Geobios* 30 (7): 977–95. [https://doi.org/10.1016/S0016-6995\(97\)80219-](https://doi.org/10.1016/S0016-6995(97)80219-7)  
440 [7](https://doi.org/10.1016/S0016-6995(97)80219-7).

441 Kidwell, Susan M. 2013. "Time-Averaging and Fidelity of Modern Death Assemblages: Building a  
442 Taphonomic Foundation for Conservation Palaeobiology." *Palaeontology* 56 (3): 487–  
443 522. <https://doi.org/10.1111/pala.12042>.

444 Kidwell, Susan M., Mairi M. R. Best, and Darrell S. Kaufman. 2005. "Taphonomic Trade-Offs in  
445 Tropical Marine Death Assemblages: Differential Time Averaging, Shell Loss, and  
446 Probable Bias in Siliciclastic vs. Carbonate Facies." *Geology* 33 (9): 729–32.  
447 <https://doi.org/10.1130/G21607.1>.

448 Kosnik, Matthew A., Quan Hua, Geraldine E. Jacobsen, Darrell S. Kaufman, and Raphael A.  
449 Wüst. 2007. "Sediment Mixing and Stratigraphic Disorder Revealed by the Age-Structure  
450 of Tellina Shells in Great Barrier Reef Sediment." *Geology* 35 (9): 811–14.  
451 <https://doi.org/10.1130/G23722A.1>.

452 Kosnik, Matthew A., Quan Hua, Darrell S. Kaufman, and Raphael A. Wüst. 2009. "Taphonomic  
453 Bias and Time-Averaging in Tropical Molluscan Death Assemblages: Differential Shell  
454 Half-Lives in Great Barrier Reef Sediment." *Paleobiology* 35 (4): 565–86.  
455 <https://doi.org/10.1666/0094-8373-35.4.565>.

456 Kowalewski, M., and R. K. Bambach. 2003. *The Limits of Paleontological Resolution*. Edited by  
457 Peter J. Harries. Springer.

458 Kowalewski, Michał. 1996. "Time-Averaging, Overcompleteness, and the Geological Record."  
459 *The Journal of Geology* 104 (3): 317–26. <https://doi.org/10.1086/629827>.

460 Kowalewski, Michał, Sahale Casebolt, Quan Hua, Katherine E. Whitacre, Darrell S. Kaufman,  
461 and Matthew A. Kosnik. 2017. "One Fossil Record, Multiple Time Resolutions: Disparate  
462 Time-Averaging of Echinoids and Mollusks on a Holocene Carbonate Platform." *Geology*  
463 46 (1): 51–54. <https://doi.org/10.1130/G39789.1>.

464 Kowalewski, Michał, Glenn A. Goodfriend, and Karl W. Flessa. 1998. "High-Resolution Estimates  
465 of Temporal Mixing within Shell Beds: The Evils and Virtues of Time-Averaging."  
466 *Paleobiology* 24 (3): 287–304. [https://doi.org/10.1666/0094-  
467 8373\(1998\)024%5B0287:HEOTMW%5D2.3.CO;2](https://doi.org/10.1666/0094-8373(1998)024%5B0287:HEOTMW%5D2.3.CO;2).

468 Kuderer, Matthias Johannes. 2022. "How Bioturbators Perturb the Paleo Record: From Eulerian  
469 to Lagrangian and Back." PhD Thesis, Utrecht University.

470 Kuderer, Matthias, and Jack J. Middelburg. 2024. "Organic Carbon Reaction Kinetics in  
471 Bioturbated Sediments." *Geophysical Research Letters* 51 (19): e2024GL110404.  
472 <https://doi.org/10.1029/2024GL110404>.

473 *MATLAB Version 25.2.0.3177638 (R2025b) Update 5*. 2025. The Mathworks, Inc.

474 Meldahl, Keith H., Karl W. Flessa, and Alan H. Cutler. 1997. "Time-Averaging and Postmortem  
475 Skeletal Survival in Benthic Fossil Assemblages: Quantitative Comparisons among  
476 Holocene Environments." *Paleobiology* 23 (2): 207–29.  
477 <https://doi.org/10.1017/S0094837300016791>.

478 Meysman, Filip, Bernard Boudreau, and Jack Middelburg. 2010. "When and Why Does  
479 Bioturbation Lead to Diffusive Mixing?" *Journal of Marine Research* 68 (6).  
480 [https://elischolar.library.yale.edu/journal\\_of\\_marine\\_research/292](https://elischolar.library.yale.edu/journal_of_marine_research/292).

481 Middelburg, Jack J., Karlina Soetaert, and Peter M. J. Herman. 1997. "Empirical Relationships for  
482 Use in Global Diagenetic Models." *Deep Sea Research Part I: Oceanographic Research  
483 Papers* 44 (2): 327–44. [https://doi.org/10.1016/S0967-0637\(96\)00101-X](https://doi.org/10.1016/S0967-0637(96)00101-X).

484 Nawrot, Rafał, Michaela Berensmeier, Ivo Gallmetzer, Alexandra Haselmair, Adam Tomašových,  
485 and Martin Zuschin. 2022. "Multiple Phyla, One Time Resolution? Similar Time Averaging  
486 in Benthic Foraminifera, Mollusk, Echinoid, Crustacean, and Otolith Fossil  
487 Assemblages." *Geology* 50 (8): 902–6. <https://doi.org/10.1130/G49970.1>.

488 Nawrot, Rafał, Martin Zuschin, Adam Tomašových, Michał Kowalewski, and Daniele Scarponi.  
489 2024. "Ideas and Perspectives: Human Impacts Alter the Marine Fossil Record."  
490 *Biogeosciences* 21 (9): 2177–88. <https://doi.org/10.5194/bg-21-2177-2024>.

491 Olszewski, T. D. 2004. "Modeling the Influence of Taphonomic Destruction, Reworking, and  
492 Burial on Time-Averaging in Fossil Accumulations." *PALAIOS* 19 (1): 39–50.  
493 [https://doi.org/10.1669/0883-1351\(2004\)019%3C0039:MTIOTD%3E2.0.CO;2](https://doi.org/10.1669/0883-1351(2004)019%3C0039:MTIOTD%3E2.0.CO;2).

494 Olszewski, Thomas. 1999. "Taking Advantage of Time-Averaging." *Paleobiology* 25 (2): 226–38.  
495 <https://doi.org/10.1017/S009483730002652X>.

496 R Core Team. 2026. *R: A Language and Environment for Statistical Computing*. R Foundation for  
497 Statistical Computing. <https://www.R-project.org/>.

498 Sadler, Peter M. 1981. "Sediment Accumulation Rates and the Completeness of Stratigraphic  
499 Sections." *The Journal of Geology* 89 (5): 569–84. <https://doi.org/10.1086/628623>.

500 Sadler, Peter M. 1993. "Models of Time-Averaging as a Maturation Process: How Soon Do  
501 Sedimentary Sections Escape Reworking?" *Short Courses in Paleontology* 6 (January):  
502 188–209. <https://doi.org/10.1017/S2475263000001112>.

- 503 Savranskaia, Tatiana, Ramon Egli, and Jean-Pierre Valet. 2022. "Multiscale Brazil Nut Effects in  
504 Bioturbated Sediment." *Scientific Reports* 12 (1): 11450.  
505 <https://doi.org/10.1038/s41598-022-14276-w>.
- 506 Scarponi, Daniele, Michele Azzarone, Kristopher Kusnerik, et al. 2017. "Systematic Vertical and  
507 Lateral Changes in Quality and Time Resolution of the Macrofossil Record: Insights from  
508 Holocene Transgressive Deposits, Po Coastal Plain, Italy." *Marine and Petroleum  
509 Geology, Sedimentology in Italy: recent advances and insights*, vol. 87 (November): 128–  
510 36. <https://doi.org/10.1016/j.marpetgeo.2017.03.031>.
- 511 Seilacher, Adolf, Luis A. Buatois, and M. Gabriela Mángano. 2005. "Trace Fossils in the  
512 Ediacaran–Cambrian Transition: Behavioral Diversification, Ecological Turnover and  
513 Environmental Shift." *Palaeogeography, Palaeoclimatology, Palaeoecology* 227 (4): 323–  
514 56. <https://doi.org/10.1016/j.palaeo.2005.06.003>.
- 515 Shull, David, and Michie Yasuda. 2001. "Size-Selective Downward Particle Transport by  
516 Cirratulid Polychaetes." *Journal of Marine Research* 59 (3).  
517 [https://elischolar.library.yale.edu/journal\\_of\\_marine\\_research/2398](https://elischolar.library.yale.edu/journal_of_marine_research/2398).
- 518 Smith, Craig R., Lisa A. Levin, Daniel J. Hoover, Gary McMurtry, and John D. Gage. 2000.  
519 "Variations in Bioturbation across the Oxygen Minimum Zone in the Northwest Arabian  
520 Sea." *Deep Sea Research Part II: Topical Studies in Oceanography* 47 (1): 227–57.  
521 [https://doi.org/10.1016/S0967-0645\(99\)00108-3](https://doi.org/10.1016/S0967-0645(99)00108-3).
- 522 Solan, Martin, Ellie R. Ward, Ellen L. White, et al. 2019. "Worldwide Measurements of  
523 Bioturbation Intensity, Ventilation Rate, and the Mixing Depth of Marine Sediments."  
524 *Scientific Data* 6 (1): 58. <https://doi.org/10.1038/s41597-019-0069-7>.
- 525 Sommerfield, Christopher K. 2006. "On Sediment Accumulation Rates and Stratigraphic  
526 Completeness: Lessons from Holocene Ocean Margins." *Continental Shelf Research*,  
527 Special Issue in Honor of Richard W. Sternberg's Contributions to Marine  
528 Sedimentology, vol. 26 (17): 2225–40. <https://doi.org/10.1016/j.csr.2006.07.015>.
- 529 Song, Shasha, Isaac R. Santos, Huaming Yu, et al. 2022. "A Global Assessment of the Mixed  
530 Layer in Coastal Sediments and Implications for Carbon Storage." *Nature  
531 Communications* 13 (1): 4903. <https://doi.org/10.1038/s41467-022-32650-0>.
- 532 Steno, Nicolaus. 1916. *The Prodomus of Nicolaus Steno's Dissertation Concerning a Solid  
533 Body Enclosed by Process of Nature within a Solid; an English Version with an  
534 Introduction and Explanatory Notes*. Vol. 4. Contributions to the History of Geology. The  
535 Macmillan company.
- 536 Sturdivant, S. Kersey, Robert J. Díaz, and George R. Cutter. 2012. "Bioturbation in a Declining  
537 Oxygen Environment, in Situ Observations from Wormcam." *PLOS ONE* 7 (4): e34539.  
538 <https://doi.org/10.1371/journal.pone.0034539>.
- 539 Tarhan, Lidya G. 2018. "The Early Paleozoic Development of Bioturbation—Evolutionary and  
540 Geobiological Consequences." *Earth-Science Reviews* 178 (March): 177–207.  
541 <https://doi.org/10.1016/j.earscirev.2018.01.011>.
- 542 Tarhan, Lidya G., Mary L. Droser, Noah J. Planavsky, and David T. Johnston. 2015. "Protracted  
543 Development of Bioturbation through the Early Palaeozoic Era." *Nature Geoscience* 8  
544 (11): 865–69. <https://doi.org/10.1038/ngeo2537>.
- 545 Tarhan, Lidya G., Kate H. Pippenger, Alison T. Cribb, et al. 2025. "Tracking Bioturbation through  
546 Time: The Evolution of the Marine Sedimentary Mixed and Transition Layers." *Science  
547 Advances* 11 (31): eadu7719. <https://doi.org/10.1126/sciadv.adu7719>.
- 548 Teal, L. R., E. R. Parker, and M. Solan. 2010. "Sediment Mixed Layer as a Proxy for Benthic  
549 Ecosystem Process and Function." *Marine Ecology Progress Series* 414: 27–40.  
550 <https://doi.org/10.3354/meps08736>.
- 551 Terry, Rebecca C., and Mark Novak. 2015. "Where Does the Time Go?: Mixing and the Depth-  
552 Dependent Distribution of Fossil Ages." *Geology* 43 (6): 487–90.  
553 <https://doi.org/10.1130/G36483.1>.

554 Tomašových, Adam, Ivo Gallmetzer, Alexandra Haselmair, et al. 2018. "Tracing the Effects of  
555 Eutrophication on Molluscan Communities in Sediment Cores: Outbreaks of an  
556 Opportunistic Species Coincide with Reduced Bioturbation and High Frequency of  
557 Hypoxia in the Adriatic Sea." *Paleobiology* 44 (4): 575–602.  
558 <https://doi.org/10.1017/pab.2018.22>.

559 Tomašových, Adam, Ivo Gallmetzer, Alexandra Haselmair, and Martin Zuschin. 2022. "Inferring  
560 Time Averaging and Hiatus Durations in the Stratigraphic Record of High-frequency  
561 Depositional Sequences." *Sedimentology* 69 (3): 1083–118.  
562 <https://doi.org/10.1111/sed.12936>.

563 Tomašových, Adam, Susan M. Kidwell, Rina Foygel Barber, and Darrell S. Kaufman. 2014. "Long-  
564 Term Accumulation of Carbonate Shells Reflects a 100-Fold Drop in Loss Rate." *Geology*  
565 42 (9): 819–22. <https://doi.org/10.1130/G35694.1>.

566 Tomašových, Adam, Susan M. Kidwell, and Ran Dai. 2023. "A Downcore Increase in Time  
567 Averaging Is the Null Expectation from the Transit of Death Assemblages through a  
568 Mixed Layer." *Paleobiology* 49 (3): 527–62. <https://doi.org/10.1017/pab.2022.42>.

569 Tomašových, Adam, Susan M. Kidwell, Ran Dai, et al. 2024. "Bioturbation Increases Time  
570 Averaging despite Promoting Shell Disintegration: A Test Using Anthropogenic Gradients  
571 in Sediment Accumulation and Burrowing on the Southern California Shelf."  
572 *Paleobiology* 50 (3): 424–51. <https://doi.org/10.1017/pab.2024.39>.

573 Tomašových, Adam, Ján Schlögl, Adrián Biroň, Natália Hudáčková, and Tomáš Mikuš. 2017.  
574 "Taphonomic Clock and Bathymetric Dependence of Cephalopod Preservation in  
575 Bathyal, Sediment-Starved Environments." *PALAIOS* 32 (3): 135–52.  
576 <https://doi.org/10.2110/palo.2016.039>.

577 Wheatcroft, Robert. 1991. "Conservative Tracer Study of Horizontal Sediment Mixing Rates in a  
578 Bathyal Basin, California Borderland." *Journal of Marine Research* 49 (3).  
579 [https://elischolar.library.yale.edu/journal\\_of\\_marine\\_research/2014](https://elischolar.library.yale.edu/journal_of_marine_research/2014).

580 Wheatcroft, Robert A. 1990. "Preservation Potential of Sedimentary Event Layers." *Geology* 18  
581 (9): 843–45. [https://doi.org/10.1130/0091-  
582 7613\(1990\)018%3C0843:PPOSEL%3E2.3.CO;2](https://doi.org/10.1130/0091-7613(1990)018%3C0843:PPOSEL%3E2.3.CO;2).

583 Wheatcroft, Robert A., and Peter A. Jumars. 1987. "Statistical Re-Analysis for Size Dependency  
584 in Deep-Sea Mixing." *Marine Geology* 77 (1): 157–63. [https://doi.org/10.1016/0025-  
585 3227\(87\)90090-9](https://doi.org/10.1016/0025-3227(87)90090-9).

586 Zhang, Shuang, Martin Solan, and Lidya Tarhan. 2024. "Global Distribution and Environmental  
587 Correlates of Marine Bioturbation." *Current Biology* 34 (12): 2580-2593.e4.  
588 <https://doi.org/10.1016/j.cub.2024.04.065>.

589 Zuhr, Alexandra M., Andrew M. Dolman, Sze Ling Ho, et al. 2022. "Age-Heterogeneity in Marine  
590 Sediments Revealed by Three-Dimensional High-Resolution Radiocarbon  
591 Measurements." *Frontiers in Earth Science* 10 (May).  
592 <https://doi.org/10.3389/feart.2022.871902>.

593